Original Article

WM&R

Waste Management & Research
2014, Vol. 32(8) 745–754
© The Author(s) 2014
Reprints and permissions:
sagepub.co.uk/journalsPermissions.nav
DOI: 10.1177/0734242X14538305
wmr.sagepub.com
SAGE

CFD analysis of municipal solid waste combustion using detailed chemical kinetic modelling

Alex Frank[1] and Marco J Castaldi[2]

Abstract

Nitrogen oxides (NO_x) emissions from the combustion of municipal solid waste (MSW) in waste-to-energy (WtE) facilities are receiving renewed attention to reduce their output further. While NO_x emissions are currently 60% below allowed limits, further reductions will decrease the air pollution control (APC) system burden and reduce consumption of NH_3. This work combines the incorporation of the GRI 3.0 mechanism as a detailed chemical kinetic model (DCKM) into a custom three-dimensional (3D) computational fluid dynamics (CFD) model fully to understand the NO_x chemistry in the above-bed burnout zones. Specifically, thermal, prompt and fuel NO formation mechanisms were evaluated for the system and a parametric study was utilized to determine the effect of varying fuel nitrogen conversion intermediates between HCN, NH_3 and NO directly. Simulation results indicate that the fuel nitrogen mechanism accounts for 92% of the total NO produced in the system with thermal and prompt mechanisms accounting for the remaining 8%. Results also show a 5% variation in final NO concentration between HCN and NH_3 inlet conditions, demonstrating that the fuel nitrogen intermediate assumed is not significant. Furthermore, the conversion ratio of fuel nitrogen to NO was 0.33, revealing that the majority of fuel nitrogen forms N_2.

Keywords

Waste-to-energy (WtE), computational fluid dynamics (CFD), waste incineration, nitrogen oxides (NO_x), furnace, boiler, ammonia (NH_3), hydrogen cyanide (HCN)

Introduction

Management of municipal solid waste (MSW) throughout the world is becoming an increasingly important focus for both individuals and municipalities. Traditionally in the United States and abroad, the majority of MSW was disposed of at landfills due to relative low cost and ease of implementation. However, in many regions, as populations and waste generation rates increase, space available for landfilling has become scarcer, and many cities have resorted to transporting MSW over large distances for disposal, requiring extensive infrastructure and energy. In recent years, there has been a shift in the research, development and implementation of alternative waste treatment technologies. Currently, conventional mass-burn waste-to-energy (WtE) facilities are one of the most prominent forms of disposal due to their high reliability, ease of operation and ability to operate consistently on a highly heterogeneous fuel.

While the emissions of WtE facilities are below permissible limits, nitrogen oxides (NO_x) continue to pose a challenge. Reduction of NO_x in combustion systems fall into two categories: primary and secondary or post-combustion. Primary reduction involves control measures such as air and fuel staging, flue gas recirculation or some combination of the two. Secondary measures use air pollution control (APC) systems to meet emission standards. In the United States, using primary and secondary control measures have succeeded in reaching NO_x levels in WtE boilers under 60 ppm (7% O_2), about 70% lower than USEPA's standard (White et al., 2009).

NO_x is a precursor to photochemical smog that is problematic in urban areas. Although it has been shown that NO_x and particulate emissions in urban areas is primarily related to automotive traffic (Ragazzi et al., 2013), any reduction that can be achieved is welcome. This will enable wider acceptance of WtE facilities near US urban centres such as the recent announcement of New York City sending an additional 725,750 tonnes of MSW per year to WTE facilities (Regan, 2013). One method to investigate and understand NO_x and pollutant formation is the use of mathematical models with two- (2D) and three-dimensional (3D) simulations. Some have focused on the combustion of the waste

[1]Department of Earth and Environmental Engineering, Columbia University, New York, USA
[2]Department of Chemical Engineering, City University of New York, New York, USA

Corresponding author:
Marco J Castaldi, Department of Chemical Engineering, City University of New York, New York, NY 10031, USA.
Email: mcastaldi@che.ccny.cuny.edu

Downloaded from wmr.sagepub.com at UCSF LIBRARY & CKM on December 13, 2014

bed (Asthana et al., 2010; Ryu et al., 2007; Yang and Swithenbank, 2008; Yang et al., 2002), while others have considered only gas-phase combustion (Huai et al., 2008; Murer et al., 2011), and a few have coupled the two together (Epelbaum and Zhang, 2007a, 2007b; Goddard et al., 2005; Nasserzadeh et al., 1991). These works have had minimal focus on nitrogen chemistry or did not address the NO_x modelling aspects completely. Yet they have been successful at predicting boiler temperature distributions and major species concentrations except NO_x.

Recognizing the complexity of NO_x chemistry, other modelling approaches have involved the use of a detailed chemical kinetic model (DCKM) in conjunction with computational fluid dynamics (CFD). A DCKM is a superior method of modelling combustion systems when intermediates are important because of the microscopic reversibility assumption of elementary reaction steps. However, due to their complexity, computational expense and convergence difficulty, they are often not utilized in real-world geometries. They are instead employed in one-dimensional (1D) or 2D perfectly stirred reactor (PSR) models that ignore transport (Rogaume et al., 2004). Although these studies provide valuable insight into the mechanisms that affect NO_x, they do not provide a realistic analysis of real-world boilers where mixing, transport and fluid dynamics play a significant role. This paper attempts to address the shortcomings of these previous models by combining the use of a DCKM in a full-scale 3D CFD model with the intent of studying NO_x chemistry. A gas-phase inlet boundary condition was utilized and adapted to study the three NO_x kinetic mechanisms: thermal (Zeldovich), prompt (Fenimore) and fuel NO. Results agree well with published works (Frank et al., 2011; Yang et al., 2007); however, this work should be considered unique for the specific boiler conditions simulated.

Theoretical basis: NO_x mechanisms

NO_x chemistry has been studied extensively in combustion and high temperature configurations. The fundamental reaction expressions with pressure and temperature dependencies have been developed for detailed chemical kinetic mechanisms. A significant body of literature can be found (Hamalainen et al., 1994; Miller and Bowman, 1989). Here a brief background on the NO_x pathways employed is presented.

Thermal NO

The thermal NO (i.e. Zeldovich) mechanism consists of a set of three coupled reactions shown in Eqs 1–3 (Turns, 2000).

$$O^* + N_2 \leftrightarrow NO + N^* \quad (1)$$

$$N^* + O_2 \leftrightarrow NO + O^* \quad (2)$$

$$N^* + OH^* \leftrightarrow NO + H^* \quad (3)$$

The thermal NO mechanism is significant at temperatures greater than 1800 K due to the high activation energy of Eq. 1. These reactions are coupled with fuel combustion through the O and OH radicals; however, the rate of Eq. 1 is slow compared with the oxidation of the fuel. Thus, thermal NO is formed in the post-combustion gases and for modelling purposes is often decoupled from the combustion reactions.

Prompt NO

The prompt (i.e. Fenimore) mechanism is intertwined with the combustion chemistry of the fuel through C, CH and CH_2 radicals described in the reaction scheme below (Miller and Bowman, 1989).

$$CH^* + N_2 \leftrightarrow HCN + N^* \quad (4)$$

$$C^* + N_2 \leftrightarrow CN^* + N^* \quad (5)$$

$$CH_2^* + N_2 \leftrightarrow HCN^* + NH^* \quad (6)$$

$$CH_2^* + N_2 \leftrightarrow H_2CN^* + N^* \quad (7)$$

Prompt NO is formed in the flame zone when hydrocarbon radicals react with molecular nitrogen from the combustion air to form cyano compounds in fuel-rich conditions. For equivalence ratios less than 1.2, hydrogen cyanide (HCN) and N are believed to be converted rapidly into NO through Reactions 8–11 (Miller and Bowman, 1989).

$$HCN + O^* \leftrightarrow NCO^* + H^* \quad (8)$$

$$NCO^* + H^* \leftrightarrow NH^* + CO \quad (9)$$

$$NH^* + H^* \leftrightarrow N^* + H_2 \quad (10)$$

$$N^* + OH^* \leftrightarrow NO + H^* \quad (11)$$

In equivalence ratios greater than 1.2, a variety of reaction pathways exist and are far more complex with myriad possible interactions. The NO concentration compared with HCN can actually decrease since the conversion of HCN in Reaction 8 is no longer rapid. Additionally, research has indicated that reactions exist where NO is 'recycled' to produce HCN and the Zeldovich mechanism can then engage with the prompt mechanism, reducing NO levels (Miller and Bowman, 1989).

Fuel NO

Most components of MSW contain some level of nitrogen with paper and plastic consisting of 0.11–0.8% and 0.3–0.85%

Downloaded from wmr.sagepub.com at UCSF LIBRARY & CKM on December 13, 2014

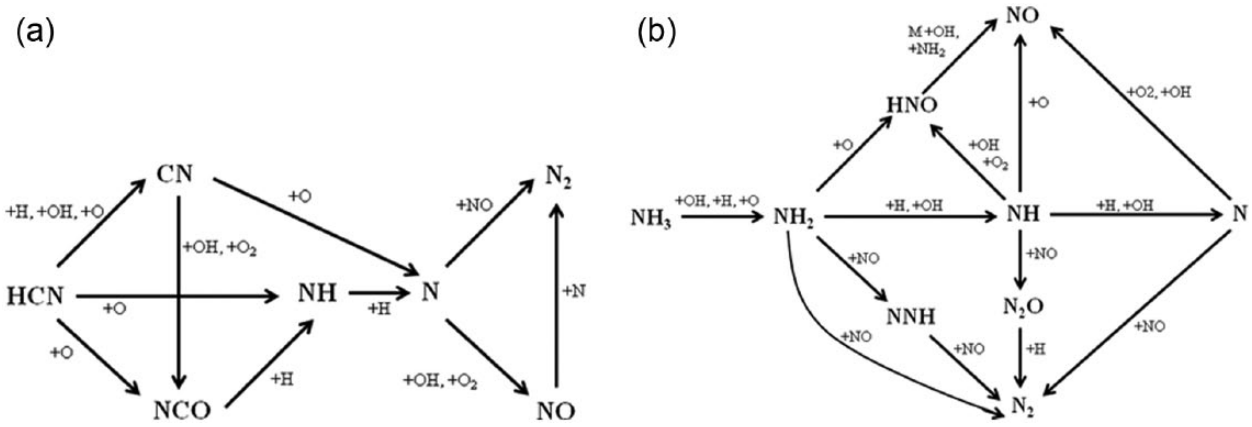

Figure 1. Reaction path for the decomposition of hydrogen cyanide (a) and ammonia (b) showing conversion to either nitrogen or NO from a fuel nitrogen source (Miller and Bowman, 1989).

nitrogen by weight, respectively (Miller and Bowman, 1989). MSW, a heterogeneous mixture, typically contains 0.5–1% nitrogen by weight while coal consists of 0.5-2.5% nitrogen by weight depending largely on the coal rank (Sorum et al., 2001). When a fuel containing nitrogen is burned, the NO released is termed 'fuel NO' and the mechanisms governing its formation are well known but have been studied mostly for coal and biomass and very minimally for MSW. During the combustion of a fuel particle, the nitrogen is distributed between the solid char matrix and the volatiles. The ratio of this distribution depends mainly on temperature and fuel structure (Sorum et al., 2001). The nitrogen released from either the char or volatiles is believed to be in four gaseous forms: ammonia (NH_3), HCN, NO or N_2. The sum of all nitrogen compounds contributing to the total NO concentration is referred to as the total fixed nitrogen (TFN) concentration and is shown by Eq. 12 (Miller and Bowman, 1989).

$$TFN = NO + NH_3 + HCN \quad (12)$$

The TFN concentration has been shown to vary significantly over a range of equivalence ratios under idealized reaction conditions with a minimum occurring under excess air conditions. Molecular nitrogen is not included in the TFN concentration, as it does not contribute to the NO produced. Inevitably, not all fuel nitrogen is released in the gaseous phase and a very small percentage, less than 0.1% (Wiles, 1996), remains in the ash after burnout has occurred.

NH_3 is believed to be the dominant fuel nitrogen product of pyrolysis from low rank fuels such as biomass, peat, lignite and low-rank coals, whereas HCN was found to be the primary fuel nitrogen compound released from bituminous coals and anthracites (Sorum et al., 2001). Hence, NH_3 appears to be the primary product when fuel nitrogen is bound in the form of amines and HCN when the fuel is bound in an aromatic ring. However, the ratio of NH_3/HCN has been shown to vary with oxygen levels, heating rates and temperatures (Glarborg et al., 2003).

The conversion of HCN has been studied extensively and a variety of reaction mechanisms have been developed. One prominent mechanism involves the reaction with oxygen radicals as shown below.

$$HCN + O^* \leftrightarrow NCO^* + H^* \quad (13)$$

$$HCN + O^* \leftrightarrow NH^* + CO \quad (14)$$

In this reaction scheme, NCO and imidogen (NH) can either combine with NO and form N_2 or on the contrary, react with an OH and O_2 forming NO. This decomposition reaction can be seen in Figure 1a (Miller and Bowman, 1989). In another study, it was found that HCN reacted primarily with OH radicals in the following reaction mechanism by Haynes, Morley and Fenimore (Miller and Bowman, 1989).

$$OH^* + HCN \leftrightarrow HOCN^* + H^* \quad (15)$$

$$OH^* + HCN \leftrightarrow CN^* + H_2O \quad (16)$$

$$CN^* + OH^* \leftrightarrow NCO^* + H^* \quad (17)$$

The products of Eq. 15 combine to form NH_2 and CO and the products of Reaction 16 react with an OH radical forming NCO and a hydrogen radical. These products then follow Reactions 9–11 finally to produce NO. It is important to note that all of the HCN produced either from prompt or fuel NO eventually form NO or N_2 thus directly increasing or decreasing the TFN concentration, respectively.

The decomposition of NH_3 and HCN are interlinked considering that one of two HCN reaction paths produces a NH* radical. One study utilizing an NH_3/oxygen flame resulted in a variety of reaction paths for the decomposition of NH_3 to either NO or N_2, which can be seen in Figure 1b.

Much like the decomposition of HCN, NH_3 forms either NO or N_2, directly changing the TFN concentration. Without discussing the individual details of the mechanism, it is clear that the local presence of oxygen plays a significant role in the NO

Downloaded from wmr.sagepub.com at UCSF LIBRARY & CKM on December 13, 2014

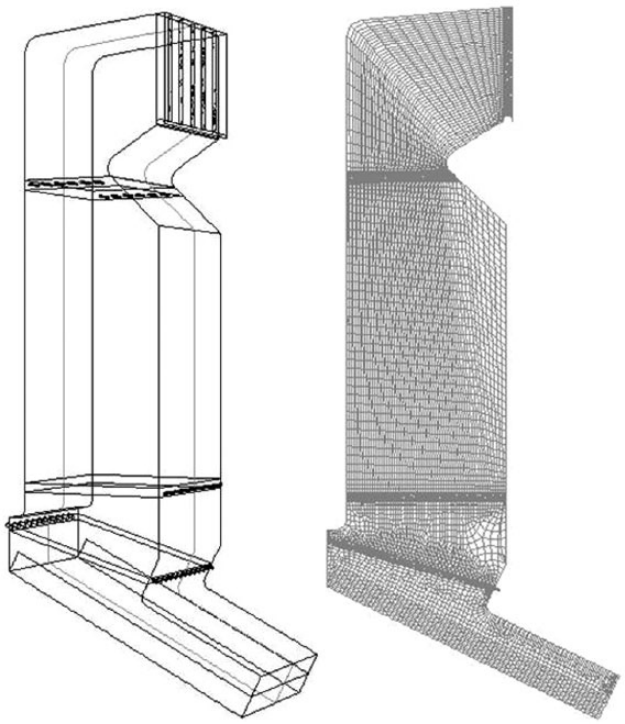

Figure 2. 3D Model geometry of waste-to-energy (WtE) boiler of the primary combustion zone (left) and computational fluid dynamics (CFD) model mesh (right) at centreline comprised of mostly hexagonal cells.

concentration considering that all paths to NO require molecular or an oxygen radical. On the other hand, all paths leading to molecular nitrogen (a reduction in TFN) require NO to be present indicating the interlinked nature of the mechanism.

Simulation methods

The CFD model developed for this study is composed of the primary combustion and radiation zone of a typical reciprocating-grate WtE boiler. The 3D model has a grate length (from waste inlet to burnout) of 8 m, a width of 4 m and a height of 17 m. The geometry contains three rows of secondary air nozzles on the front and rear walls along with a row of tertiary nozzles on the side walls of the boiler at a height of 12 m. The tertiary nozzles typically serve as the primary injection of NO reductant and a means to quench the flame; however, for the studies presented, this flow was not enabled, as NO reduction through selective non-catalytic reduction (SNCR) was not of interest. The model geometry was constructed in Unigraphics (Siemens PLM, Plano, TX, USA) and the hex-dominant mesh of about 800 000 cells was created in ANSYS Workbench (ANSYS Inc., Canonsburg, PA, USA); both can be seen in Figure 2. The mesh size was optimized for both solution fidelity while maintaining a reasonable solution time with a DCKM. Simulations were initially performed with a high-resolution mesh of 3.4 million cells and compared with the current 800 000 cell mesh, which showed agreement of all outlet species within 5%. The commercial code FLUENT 13.0 was employed to run the fluid simulation due to its robustness in modelling flow with complex chemistry. Furthermore, salient model boundary conditions can be seen in Table 1. It must be noted that radiation was not considered in the model, a simplification that will have little impact on nitrogen chemistry, the primary focus of this study.

Table 1. Computational fluid dynamics (CFD) model setting details.

Model mesh	800,000 cell hex dominant
Solver settings	Steady state, pressure based with gravity enabled, compressible flow
Turbulence model	Realizable K-epsilon with standard wall function
Reaction model	Eddy dissipation concept with 50 species, 309 reaction DCKM
Primary inlet boundary conditions	Above-grate gas-phase empirical model consisting of mass flow, temperature and species concentration (flow rate of 11.9 kg s^{-1})
Secondary air inlet boundary conditions	Three rows of jets injecting ambient air (flow rate of 8 kg s^{-1})
Wall boundary conditions	Adiabatic (acceptable for parametric study of NO_x), temp. of 273 K

DCKM, detailed chemical kinetic model.

Table 2. Waste boundary condition composition (Murer et al., 2011).

	Mass % (dry)
Water	24.25
Ash	19.10
Carbon	32.38
Hydrogen	4.54
Oxygen	19.05
Nitrogen	0.68

The quality and accuracy of any CFD simulation is directly determined by fidelity of the boundary conditions utilized. For the waste bed inlet condition, an extensively validated fuel conversion model based on the Amsterdam plant in the Netherlands (Murer et al., 2011) was used to generate the gas-phase inlet profile. The model considered German MSW and the composition details are shown in Table 2. The total throughput of fuel is 6980 kg h^{-1} with a lower heating value of 12 935 kJ kg^{-1}, which results in a total energy release of approximately 26 MW including radiation, chemical energy and sensible heat. In developing the inlet boundary condition, an extensive amount of details was considered. First, the primary air flow through the grate was divided into five equally spaced zones that correspond to the four stages of waste decomposition: drying, pyrolysis, gasification and char burnout. Conserving mass and energy, profiles for mass flow, temperature and seven product species were developed to model the burning waste bed, including CO, CO_2, H_2, O_2, H_2O, N_2 and lastly a fuel nitrogen intermediate of HCN or NH_3, considered while keeping the TFN constant. The fuel nitrogen intermediate

Downloaded from wmr.sagepub.com at UCSF LIBRARY & CKM on December 13, 2014

is considered released within the first 30% of the grate during the drying and pyrolysis of the fuel. This is consistent with previous studies (Glarborg et al., 2003) involving biofuels and low rank coals that showed release of over 80% of their fuel nitrogen in temperature ranges of 850–900 C, a value that is exceeded in this region of the boiler. Since fuel nitrogen is of high importance in this study, a variety of conversion products were considered and will be discussed in detail in the results section. Profiles for temperature, species mass decomposition, mass flow and a few select species concentrations are shown in Figure 3. From the figures, it can be noted that the profile of all species, temperature and mass across the waste inlet is not uniform, a result of a randomizing algorithm to represent the heterogeneous composition of the burning waste bed.

In order to model the complexities of nitrogen chemistry, a well-known and comprehensive DCKM was utilized, the GRI 3.0, containing 325 reaction steps and 53 species (Smith et al., 2013). Three species – Ar, C_3H_7 and C_3H_8 – were removed including their reactions due to the limitation of 50 species in FLUENT, thus making the mechanism 50 species and 309 steps. The GRI 3.0 includes all combustion reactions and the mechanisms for nitrogen chemistry, thereby making it suitable for this study.

Simulation results

Case 1: N_2 inlet boundary condition model

The first step to validating the CFD model is to ensure that the simulation is in good agreement with existing boiler data for temperature, flow distribution and species concentration. Before a DCKM was used as the representative combustion model, the CFD model was first validated with a set of global combustion reactions (Frank et al., 2011), which matched test data well. Switching to the DCKM provided similar results for temperature and species concentrations (not considering NO_x), which demonstrates the proper functioning of the model.

Figure 4a shows a temperature contour plot at the boiler centreline with the flow being pushed towards the front wall a few feet above the grate, a result that is consistent with the offset of secondary air nozzles between front and rear walls, with the front containing one and the rear containing two rows. The peak temperature of 2170 K occurs in the centre of the boiler in the area of secondary air impingement into the burning fuel. This peak temperature is about 20% higher than previous works (Murer et al., 2011), which is expected due to the non-uniform flow distribution and adiabatic wall boundary condition.

Furthermore, contours of CO, O_2, H_2O and CO_2 can be seen in Figures 4b–e. The contour plot of CO shows that the high concentration coming off the bed is oxidized quickly, resulting in an output concentration of 45 ppmdv (7% O_2), a reasonable value that agrees with previous results (Yang et al., 2007). It is evident that the lack of oxygen available for oxidation of CO in the lower portion of the boiler leads to the higher concentration in this area. The immediate introduction of oxygen via secondary air clearly reduces the CO concentration to a near zero value. The contour plot of O_2 shows an area of deficiency in the lower portion of the boiler near the waste inlet and a strong concentration along the rear wall. Ideally, this concentration would be more uniform but the optimization of secondary air distribution was not the goal of this study. The contour plot of water shows a high concentration at the wet waste inlet, which travels along the front wall, consistent with the inlet profile. When the waste first enters the bed, drying immediately occurs, resulting in the distribution shown. Lastly, the concentration plot of CO_2 depicts a high concentration directly in the centre of the grate where the complete combustion of the waste is occurring. This peak concentration quickly becomes diluted by the secondary air and is pushed towards the front wall, consistent with the other constituents. The comparison of these results to existing data and other studies show the fidelity of the CFD model.

Next, we consider NO chemistry, which is a very complex portion of the model details. To determine which NO intermediate is most appropriate for the simulation, a series of parametric studies were undertaken. First, to determine boiler concentrations of prompt and thermal NO without the influence of fuel nitrogen, an inlet boundary condition was generated considering 100% conversion of fuel nitrogen to molecular nitrogen, essentially making it inert. For this case, a contour plot of NO is shown in Figure 5a where the boiler outlet concentration is 80 ppmdv (7% O_2). NO is the primary NO_x species emitted with NO_2 and N_2O accounting for less than 1 ppmdv combined and therefore only NO will be discussed further. The figure shows the highest concentration occurring in the mixing zone, near the highest temperature in the boiler indicating the importance of the Zeldovich mechanism. The expected concentration of NO without any secondary abatement is expected to be approximately 300 ppmdv (White et al., 2009), thus indicating that while significant to the total NO contribution, thermal and prompt mechanisms do not account for the majority of the NO generated in the system. It is also worth noting that the NO values presented are a worst-case result as the elevated temperature and therefore reduced residence time would produce the highest achievable thermal NO concentration in the boiler.

In order to determine the most pertinent reactions in the formation of NO, contours of the net rate of reaction of NO were plotted and can be seen in Figure 5b. The plot illustrates the highest rate occurring in the area of highest concentration of NO indicating that the majority of NO is formed in this location. To determine the individual reactions that are most significant, contours of each reaction rate were plotted and compared with the contours of the net rate. The reaction plots with high concentrations that most similarly match the net rate plots are therefore the most significant. Results indicate the importance of the thermal mechanism with Eq. 1 being the most significant with the highest rate of 2.95×10^{-5} kgmol s^{-1} m^{-3}, followed closely by Eqs 3 and 2 with rates of 2.24×10^{-5} and 1.40×10^{-5}, respectively. All of the maximum rates occur in close proximity to the maximum

Downloaded from wmr.sagepub.com at UCSF LIBRARY & CKM on December 13, 2014

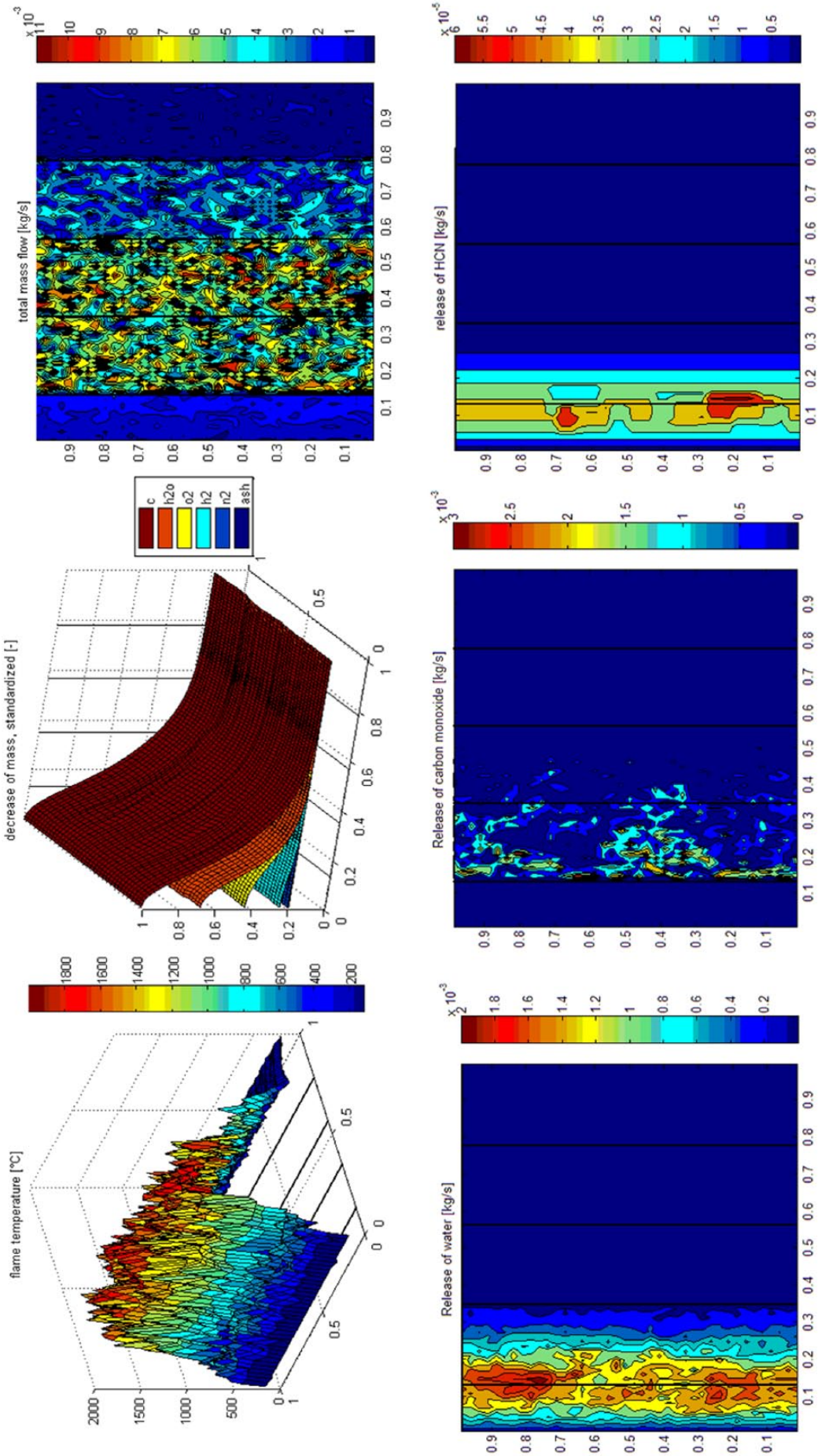

Figure 3. Computational fluid dynamics (CFD) model inlet boundary conditions with position normalized along the grate length and width. Temperature profile (top left) in C with waste inlet on front left surface, profile of inlet municipal solid waste (MSW) mass decomposition (top centre) and profiles of mass flow in kg s^{-1} (top right), water, carbon monoxide and hydrogen cyanide (fuel nitrogen intermediate), all with the waste inlet on the left side and waste burnout on the right.

Downloaded from wmr.sagepub.com at UCSF LIBRARY & CKM on December 13, 2014

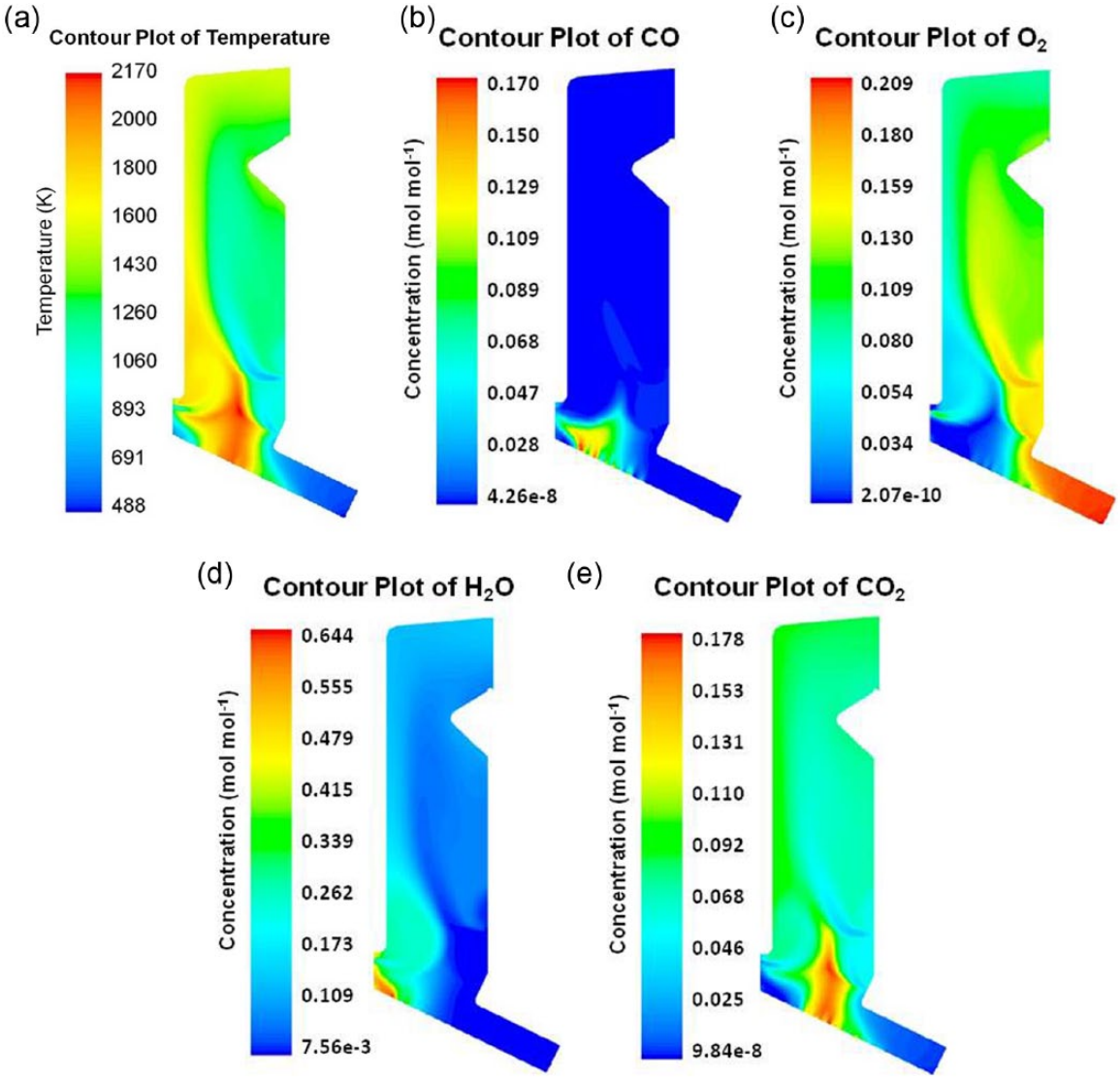

Figure 4. Contour plots of temperature at the boiler centreline (a) with the maximum of 2170 K occurring above the grate with secondary air pushing the flow towards the front wall, CO concentration (b) showing quick oxidation directly above the grate, O_2 (c) showing high concentration on rear wall, H_2O (d) detailing a high concentration near the waste inlet and lastly, contours of CO_2 (e) with the highest concentration in the centre of the boiler, during the pyrolysis and burning of the fuel.

concentration of NO in the boiler. Prompt NO also plays an important, albeit smaller role in the formation of NO with maximum rate being two orders of magnitude smaller than the thermal mechanism. Also worth noting is that the interaction of secondary air into this area produces a negative rate indicating that atomic oxygen is reducing the NO.

Case 2: HCN inlet boundary condition model

In order to determine the most appropriate fuel nitrogen intermediate, the model inlet boundary condition was modified to consider complete conversion of fuel nitrogen to HCN. The HCN is assumed released very early in the pyrolysis of the fuel (see Figure 3) and contributes very minimally to the total heat release. Results for temperature, O_2 and H_2O are identical to case 1. However, exit CO concentrations are approximately double indicating that the change in fuel nitrogen boundary condition does have an impact on fuel carbon chemistry. Figure 1a and Eq. 14 detail that HCN can produce CO; therefore the increase in concentration is expected.

NO exit concentration is markedly higher at 989 ppmdv (7% O_2) with N_2O and NO_2 having exit concentrations of 1 and 8 ppmdv, respectively. The contour of NO concentration is shown in Figure 5c. The highest concentration is located along the front wall near the secondary air inlet indicating that both air and turbulence may play a significant role in NO production. It is worth noting that the highest temperature region does not show a significant concentration of NO illustrating that the incoming HCN is dominant compared with the thermal mechanism. The concentration of NO is significantly higher than expected in a typical WtE boiler showing that full conversion of fuel nitrogen to HCN is not likely. Excluding the thermal and prompt NO results obtained in case 1, it can be assumed that 908 ppmdv (7% O_2) are

Downloaded from wmr.sagepub.com at UCSF LIBRARY & CKM on December 13, 2014

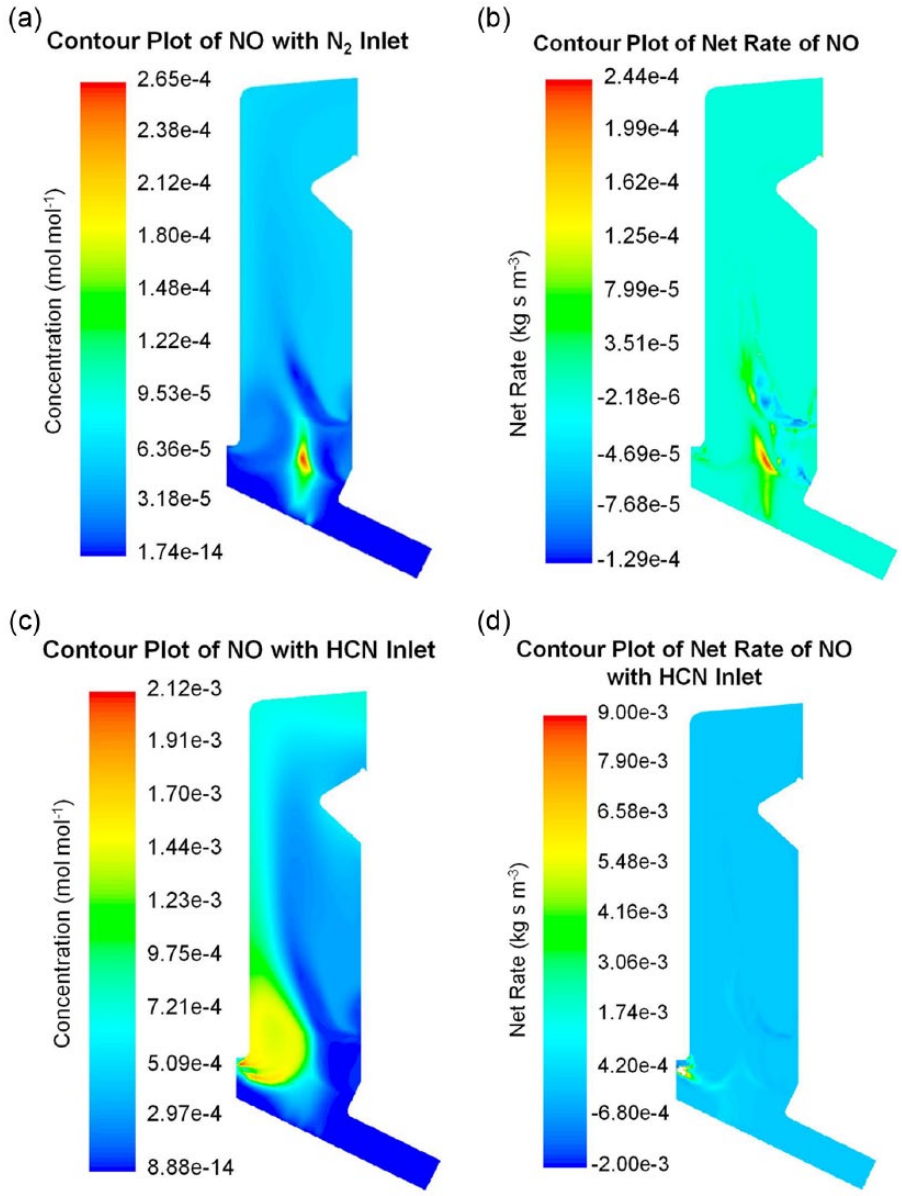

Figure 5. Contour plots at the boiler centreline of NO concentration (a) and net rate of reaction of NO (b) for case 1 where NO exhibits a high concentration above the grate near the highest temperature region of the boiler which quickly mixes and becomes uniform in the upper portion of the boiler. Contour plot of net rate of reaction of NO depicts the maximum rate occurring near the area of highest temperature above the grate. Negative rates from secondary air injection illustrate reduction of NO. Contour plots of NO concentration (c) and net rate of reaction of NO (d) for case 2 at the boiler centreline where the highest concentration of NO exists on the front wall near secondary air injection. The maximum rate occurs towards the front wall at the secondary air inlet.

released from HCN since there is a near zero exit concentration of HCN.

In order to match the expected 300 ppmdv results, the conversion factor of fuel nitrogen to NO would have to be approximately 33%. This value is consistent with previous research by Sorum et al. (2001), who discovered that conversion rates ranged from 23% to 99% depending on oxygen levels for varying types of individual MSW paper components. For plastics, it was much more difficult to obtain a direct fuel nitrogen conversion measurement, as the temperature levels and thus NO concentrations were elevated generating high levels of thermal NO. Conversion rates in these cases were over 1000% indicating that the majority of NO was generated from non-fuel nitrogen. In these experiments, only individual components were burned in the reactor but when mixtures of plastics and papers were tested together, fuel nitrogen to NO conversion were lower in all cases. Furthermore, other experiments proved that varying the ratio of the components of the mixtures could change the outlet NO concentration by up to 50%. These experimental results detail the extremely complex nature of NO chemistry even in a very controlled environment.

Examining the mechanism in detail, the net rate of NO at the centreline for case 2 can be seen in Figure 5d. In this case, a high rate can be seen near the front wall secondary air inlet, which is

Downloaded from wmr.sagepub.com at UCSF LIBRARY & CKM on December 13, 2014

consistent with the high NO concentration in this area and upstream along the front wall. Individual reaction rates in this area indicate that HNO is the most important species, which reacts with H and OH radicals by Eqs 18 and 19 with the former having the largest effect.

$$HNO^* + H^* \leftrightarrow H_2 + NO \quad (18)$$

$$HNO^* + OH^* \leftrightarrow NO + H_2O \quad (19)$$

Furthermore, NCO is a significant species and forms NO by Eq. 20 below.

$$NCO^* + O^* \leftrightarrow NO + CO \quad (20)$$

Both of these key compounds, HNO and NCO, can be seen as important species in Figure 1 that directly form NO. It is also important to note that it is necessary to have O, H and OH radicals in order to have these reactions occur.

Case 3: NH_3 inlet boundary condition model

The last fuel nitrogen intermediate considered is NH_3, where similar to case 2, complete conversion of fuel nitrogen is assumed. The exit concentration is slightly lower but very close to case 2 at 938 ppmdv (7% O_2), a somewhat surprising result considering the NO reduction properties of NH_3. This reduction in 51 ppm or about 5% compared with case 2 is fairly insignificant and shows the fuel nitrogen intermediate that is assumed is not very significant. Contour plots of both NO concentration and the net rate are nearly identical to case 3, demonstrating the similarities between the two cases. Further examination reveals that the same two reactions, Eqs 18 and 19, play the largest role in the production of NO, following the reaction path shown in Figure 1b. Unlike case 2, the exit CO concentration is the same as case 1 at 45 ppmdv, further proving that the presence of HCN does directly increase the concentration of CO in the boiler.

Case 4: HCN, NH_3 and NO inlet boundary condition model

Since results for both HCN and NH_3 provided very similar NO concentrations, it is therefore not possible to determine which fuel nitrogen intermediate is most likely to occur in the system. Measurements taken on a pilot scale MSWI reported the presence of only NH_3 up to 2000 mg Nm^{-3} (Hunsinger, 2010). Based on cases 2 and 3, it is also not clear whether any interaction between the species exists and would affect the concentration of NO. In order to determine this result, a case was run considering equal division among three fuel nitrogen intermediates- HCN, NH_3 and NO being released directly from the bed. The results from this case show an outlet NO concentration of 970 ppmdv (7% O_2), a value directly between cases 2 and 3. This proves the interaction between fuel nitrogen intermediates and NO is very minor. In considering NO being released directly from the bed, there was also consideration of NH_3 reduction of NO but this proved not to be significant. The results from all four cases prove there is little to no importance given to the assumed fuel-nitrogen intermediate as all produce nearly identical NO concentrations regardless of the path in which it is formed.

Conclusions

A study was performed aimed at studying the mechanisms governing the formation of NO_x in WtE systems by utilizing CFD coupled with a DCKM. The 0.8 million cell model consisting of the primary combustion zone of a typical boiler was first validated with an inert fuel nitrogen inlet combined with a well validated inlet boundary condition. Results matched previous research very well indicating the fidelity of the model.

A parametric study varying the fuel nitrogen inlet boundary conditions was used to determine the most realistic fuel-nitrogen intermediate. Results have shown that fuel nitrogen to NO conversion is about 33% and that either HCN, NH_3 or NO all provide exit NO concentrations within 5% of each other. Therefore the assumption for fuel nitrogen intermediate is not significant to the final NO concentration for this particular case study.

Declaration of conflicting interests

The authors declare that there is no conflict of interest.

Funding

This research received no specific grant from any funding agency in the public, commercial, or not-for-profit sectors.

References

Asthana A, Menard Y, Sessiecq P and Pattison F (2010) Modeling on-grate MSW incineration with experimental validation in a batch incinerator. *Industrial & Engineering Chemistry Research* 49: 7597–7604.

Epelbaum G and Zhang H (2007a) Process simulation of a large mass burn waste-to-energy boiler by the combination of CFD software programs. *Progress in Computational Fluid Dynamics* 7: 11–18.

Epelbaum G and Zhang H (2007b) New development in EfW process modeling: fully integrated CFD model. In: *Proceedings of the North American Waste to Energy Conference*, Miami, FL, 21–23 May, pp. 85–95.

Frank A, Castaldi MJ and Nakamura MR (2011) Numerical modeling of pollutant formation in waste-to-energy systems using computational fluid dynamics. In: *Proceedings of the North American Waste to Energy Conference*, Lancaster, PA, 16–18 May, pp. 43–46.

Glarborg P, Jensen AD and Johnsson JE (2003) Fuel nitrogen conversion in solid fuel fired systems. *Progress in Energy and Combustion Science* 29: 89–113.

Goddard CD, Yang YB, Goodfellow J, Sharifi VN, Swithenbank J, Chartier J, Mouquet D, Kirkman R, Barlow D and Moseley S (2005) Optimisation study of a large waste-to-energy plant using computational modeling and experimental measures. *Journal of the Energy Institute* 78: 106–111.

Hamalainen JP, Aho MJ, Tummavuori J (1994) Formation of nitrogen oxidizes from fuel-N through HCN and NH3: a model-compound study. *Fuel* 73: 1894–1898.

Huai XL, Xu WL, Qu ZY, Li ZG, Zhang FP, Ziang GM, Zhu SY and Chen G (2008) Analysis and optimization of municipal solid waste combustion in a reciprocating incinerator. *Chemical Engineering Science* 63: 3100–3113.

Downloaded from wmr.sagepub.com at UCSF LIBRARY & CKM on December 13, 2014

Hunsinger H (2010) A new technology for high efficient waste-to-energy plants. In: *2nd W2W & 6th I-CIPEC Conference*, Kuala Lumpur, 26–29 July.

Miller JA and Bowman CT (1989) Mechanism and modeling of nitrogen chemistry in combustion. *Progress in Energy and Combustion Science* 15: 287–338.

Murer M, Spleithoff H, de Waal CMW, Wilpshaar S, Berkhout B, van Berlo MAJ, Gohlke O and Martin JJE (2011) High efficient waste-to-energy in Amsterdam: getting ready for the next steps. *Waste Management & Research* 29: 20–29.

Nasserzadeh V, Swithenbank J and Jones B (1991) Three-dimensional modeling of a municipal solid-waste incinerator. *Journal of the Institute of Energy* 64: 166–175.

Ragazzi M, Tirler W, Angelucci G, Zardi D and Rara EC (2013) Management of atmospheric pollutants from waste incineration processes: the case of Bozen. *Waste Management & Research* 31: 235–240.

Regan J (2013) Covanta Energy, http://www.covantaenergy.com/en/news/press-releases/2013/Copy%20of%20aug-19.aspx.

Rogaume T, Richard F and Jabouille F (2004) Computational model to investigate the mechanisms of NO_x formation during waste incineration. *Combustion Science and Technology* 176: 925–943.

Ryu C, Phan AN, Yang Y, Sharifi VN and Swithenbank J (2007) Ignition and burning rates of segregated waste combustion in packed beds. *Waste Management* 27: 802–810.

Smith G, Golden D, Frenklach M, Moriarty NW, Eiteneer B, Goldenberg M, Bowman CT, Hanson RK, Song S, Gardiner WC, Lissianski VV and Qin Z (2013) http://www.me.berkeley.edu/gri_mech/ (17 August 2013).

Sorum L, Skreiberg O, Glarborg P, Jensen A and Dam-Johansen K (2001) Formation of NO from combustion of volatiles from municipal solid wastes. *Combustion and Flame* 123: 195–212.

Turns SR (2000) In: Holman JP and Lloyd J (eds) *An Introduction to Combustion: Concepts and Applications*. 2nd ed. Boston, MA: McGraw-Hill, pp. 168–171.

White M, Goff S, Deduck S and Gohlke O (2009) New process for achieving very low NO_x. In: *Proceedings of the North American Waste to Energy Conference*, Chantilly, VA, 18–20 May, pp. 83–87.

Wiles C (1996) Municipal solid waste combustion ash: state-of-the-knowledge. *Journal of Hazardous Materials* 47: 325–344.

Yang YB and Swithenbank J (2008) Mathematical modelling of particle mixing effect on the combustion of municipal solid wastes in a packed-bed furnace. *Waste Management* 28: 1290–1300.

Yang YB, Nasserzadeh V, Goodfellow J, Goh YR and Swithenbank J (2002) Parameter study on the incineration of municipal solid waste fuels in packed beds. *Journal of the Institute of Energy* 75: 66–80.

Yang YB, Sharifi VN and Swithenbank J (2007) Converting moving-grate incineration from combustion to gasification – numerical simulation of burning characteristics. *Waste Management* 27: 645–655.

Downloaded from wmr.sagepub.com at UCSF LIBRARY & CKM on December 13, 2014